ASSOCIAZIONE NAZIONALE ITALIANA DI INGEGNERIA SISMICA
ANIDIS
Italian National Association of Earthquake Engineering

XVIII CONVEGNO ANIDIS
L'ingegneria sismica in Italia
ASCOLI PICENO 2019
15-19 Settembre

Shake-table investigation of a timber retrofit solution for unreinforced masonry cavity-wall buildings

Marco Miglietta[a], Nicolò Damiani[a], Luca Grottoli[b], Gabriele Guerrini[b,c], Francesco Graziotti[b,c]
[a] *UME Graduate School, IUSS Pavia, Piazza della Vittoria 15, 27100 Pavia, Italy*
[b] *European Centre for Training and Research in Earthquake Engineering (EUCENTRE), via Ferrata 1, 27100 Pavia, Italy*
[c] *Dept. of Civil Engineering and Architecture (DICAr), University of Pavia, via Ferrata 3, 27100 Pavia, Italy*

Keywords: Unreinforced masonry, cavity walls, full-scale shaking-table test, timber retrofit system, damage limit states, timber flexible diaphragm

ABSTRACT
Two unreinforced masonry full-scale building prototypes with identical geometrical features were tested dynamically on the shake-table at the EUCENTRE laboratories in Pavia, one in its bare conditions and one in retrofitted configuration, within a comprehensive research campaign on the vulnerability of existing Dutch structures. The tested buildings represented the end-unit of a two-storey terraced house typical of the Groningen region of The Netherlands, which has been recently affected by induced seismicity due to gas extraction. The original structural system consists of cavity walls without any particular seismic design or detailing. The prototypes included two storeys, with a reinforced concrete slab at the first floor, a flexible timber diaphragm at the second one and a pitched timber roof supported by two gable walls. The retrofit system consisted of timber frames mechanically connected to the building piers and floors, on which oriented-strand boards were nailed. The incremental dynamic tests were performed up to the near-collapse conditions of the two specimens, using the same input motion representative of Groningen induced seismicity. This paper describes the characteristics of the tested buildings and compares the observed damage patterns.

1 INTRODUCTION

The experimental tests presented in this paper are part of a wide experimental campaign aiming at the seismic risk assessment of the Groningen region, in the North-Eastern part of The Netherlands (Bommer et al. 2015, Bourne et al. 2015, Crowley et al. 2018, van Elk 2019). The area has been exposed to induced seismicity due to gas extraction during the last decades.

Since a complete seismic risk assessment requires an understanding of the existing building responses to seismic actions, a large experimental campaign was launched in 2014 at the EUCENTRE laboratories in Pavia (Italy) to investigate the seismic behavior of Dutch unreinforced masonry (URM) buildings subjected to earthquake loading (Graziotti et al. 2018). The campaign included: static or quasi-static test on materials, masonry assemblies and structural components (Graziotti et al. 2016a); dynamic shake-table tests on entire buildings (Graziotti et al. 2017; Kallioras et al. 2018) or sub-systems (Graziotti et al. 2016b, Graziotti et al. 2019); and analytical studies (Malomo et al. 2018; Tomassetti et al. 2018; Kallioras et al. 2019). At the same time, an extensive experimental campaign was launched also at the Delft University of Technology (The Netherlands) (Jafari et al. 2017; Messali et al. 2017; Rots et al. 2017).

The building typology investigated within the present work is Dutch terraced house of the late 1970s, a residential class recognized to be particularly vulnerable to earthquakes. Aiming at investigating a new light strengthening system, two identical full-scale replicas of a terraced house end-unit, one in bare conditions (Miglietta et al. 2018) and one in retrofitted configuration (Damiani et al. 2019), were subjected to the same unidirectional incremental dynamic test up to their near collapse state at the EUCENTRE laboratories.

This paper briefly compares the observed damage patterns obtained with the two shaking-

table tests. All processed data are freely available upon request at http://www.eucentre.it/nam-project.

2 SPECIMEN OVERVIEW

2.1 Geometry and construction details

The prototype buildings were two identical full-scale replicas of a typical Dutch terraced house end-unit (Figure 1). They were characterized by a URM cavity-wall structural system consisting of a 100-mm-thick load-bearing single-wythe calcium silicate (CS) inner-leaf and a 100-mm-thick external single-wythe clay veneer, separated by an air-gap of approximately 80 mm. Being such building typology typically composed by adjacent units with independent load-bearing and floor systems and continuous exterior veneers, the choice of testing an end-unit was taken in order to investigate also the out-of-plane response of cavity-walls under seismic excitation (Figure 2, North façade).

The prototypes were 5.9-m long and 5.6-m wide, built on a rigid foundation fixed to the shake-table (Figure 2). The longitudinal East and West sides were characterised by the typical length found in situ and were oriented parallel to the shaking direction (Figure 3). The transverse dimensions (North and South sides) were slightly reduced compared to actual buildings due to shake-table and laboratory constrains. Figure 4 and Figure 5 show the four elevations of the calcium-silicate inner-leaf.

The specimens included a 150-mm-thick reinforced concrete (RC) slab at the first floor. A flexible timber diaphragm was provided at the second floor, composed by 100x240-mm timber joists and 18-mm-thick, 185-mm-wide tongue-and-groove nailed planks. A 39° pitched timber roof made of 100x240-mm purlins and 18-mm-thick, 185-mm-wide tongue-and-groove nailed planks completed the building. Both floor diaphragms presented a staircase hole on the North side (Figure 3b).

The prototype longitudinal East and West façades were characterized by large openings, asymmetrically distributed throughout the building, resulting in several very slender piers. Two squat piers were present, one on the East side at the first storey and one on the West side at the second storey (Figure 2 through Figure 4).

Inner and outer leaves were linked by 200-mm-long steel ties with a diameter of 3.1 mm, distributed with a density of 1 tie/m^2 to simulate in-situ degraded conditions (Figure 4, Figure 5 and Figure 6a). The 5.75-m-long second floor and roof timber beams were oriented parallel to the shaking direction and supported only by transverse CS internal walls (Figure 6b). The connection between beams and walls were improved by L-shape steel anchors screwed to the beams, which anchored them passing through the width of the walls (Figure 6b).

Figure 1. Typical terraced house in Groningen: front façade with highlighted end-unit.

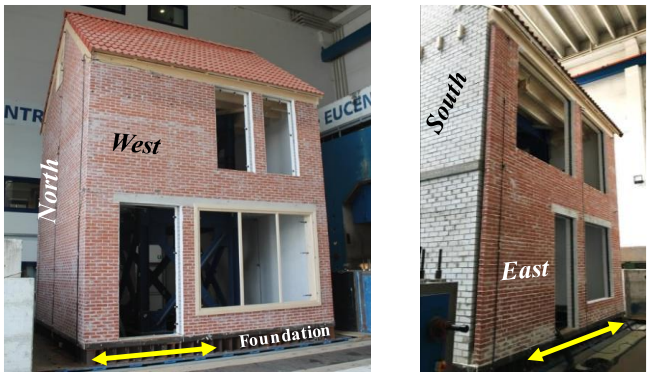

Figure 2. Building prototypes after completion; yellow arrows indicate the shaking direction.

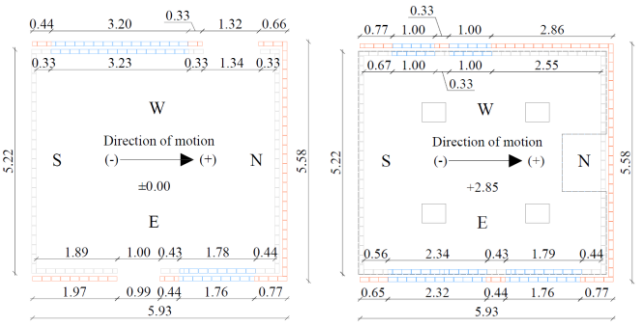

a) b)

Figure 3. Plan views of the prototypes: a) first storey; b) second storey. Units of m.

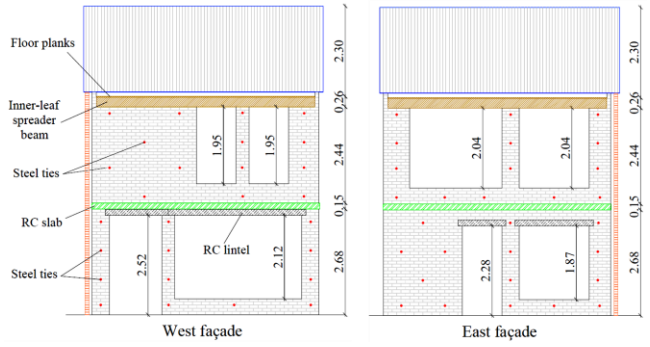

Figure 4. Calcium silicate longitudinal walls: elevations from outside. Units of m.

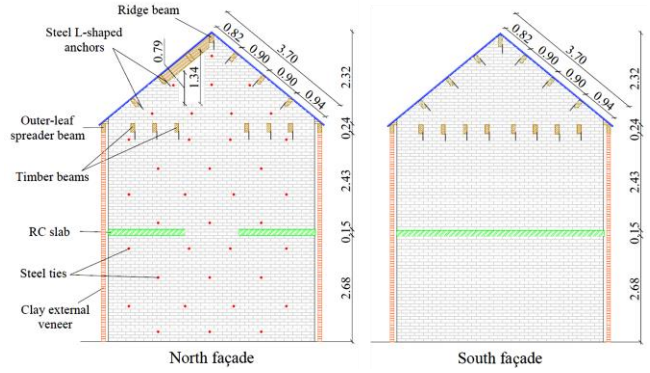

Figure 5. Calcium silicate transverse walls: elevations from outside. Units of m.

a) b)

Figure 6. Connection details: a) inner-to-outer leaf with steel ties; b) timber beams-to-transverse walls with L-shape steel anchors.

2.2 Retrofit system details

The proposed retrofit system was conceived considering a low impact, sustainable and reversible intervention. It aimed at improving four aspects of the bare building prototype structural system: (i) the walls out-of-plane resistance; (ii) the walls in-plane capacity; (iii) the stiffness of the second floor timber diaphragm; and (iv) the connections between walls and floor systems.

The out-of-plane capacity of transverse walls (North and South sides) was enhanced through the application of 80x60-mm timber vertical posts (also termed strong-backs), where the smaller dimension was oriented perpendicular to the masonry walls. They were spaced at approximately 600 mm, mechanically fastened to the masonry through steel angles (Figure 7). Top and bottom timber sill-plates with the same section allowed the connection between timber posts and floor diaphragms or foundations (Figure 7, Figure 8 and Figure 9).

To increase the in-plane capacity of piers, tie-down anchors and horizontal blocking elements were added to the out-of-plane retrofit system, creating a frame with flexural capacity. 18-mm-thick oriented-strand boards (OSB) were nailed to the timber frame to increase also the shear capacity (Figure 7), driven by the American recommendations for timber shear-walls (AWC 2008).

The second-floor timber diaphragm was stiffened by nailing 18-mm-thick OSB panels on it, following the American standards for timber diaphragms (AWC 2008). Timber blocking with a section of 100x240 mm were inserted between the beams to allow nailing the OSB panels along all our sides (Figure 10).

The improvement of the connections between masonry walls and the first-floor slab was obtained by fastening the first-storey top sill-plates through the RC slab to the second-storey bottom sill plates using ∅12 threaded bars (Figure 8).

The connection between longitudinal walls and second floor diaphragm were improved screwing at about 150-mm spacing the second-storey top sill-plates to the inner-leaf spreader beams. The OSB panels added to the second-floor diaphragm were also nailed to the inner-leaf spreader beam through the existing planks (Figure 9a).

The connections between transverse walls and timber floor were improved by inserting timber blocking between beams and screwing to them the second-storey timber top sill-plates and attic bottom sill-plates at about 100-mm spacing (Figure 9b and Figure 10).

Moreover, coupling between inner and outer leaves was enhanced increasing the density of steel ties to 5 ties/m^2.

2.3 Masses

Calcium silicate and clay masonry were characterized by a density of 1850 kg/m^3 and 2020 kg/m^3, respectively. The thickness of the first-floor RC slab was chosen to include also live loads, with a total mass of 11.2 t. The second-floor timber diaphragm mass was about 700 kg, with an additional mass of 1.2 t to simulate live loads. The roof timber structure had a mass of 700 kg, with additional 2.1 t of tiles.

The total weight of the bare building prototype was 47.5 t, while the one of the retrofitted specimen was 49.1 t.

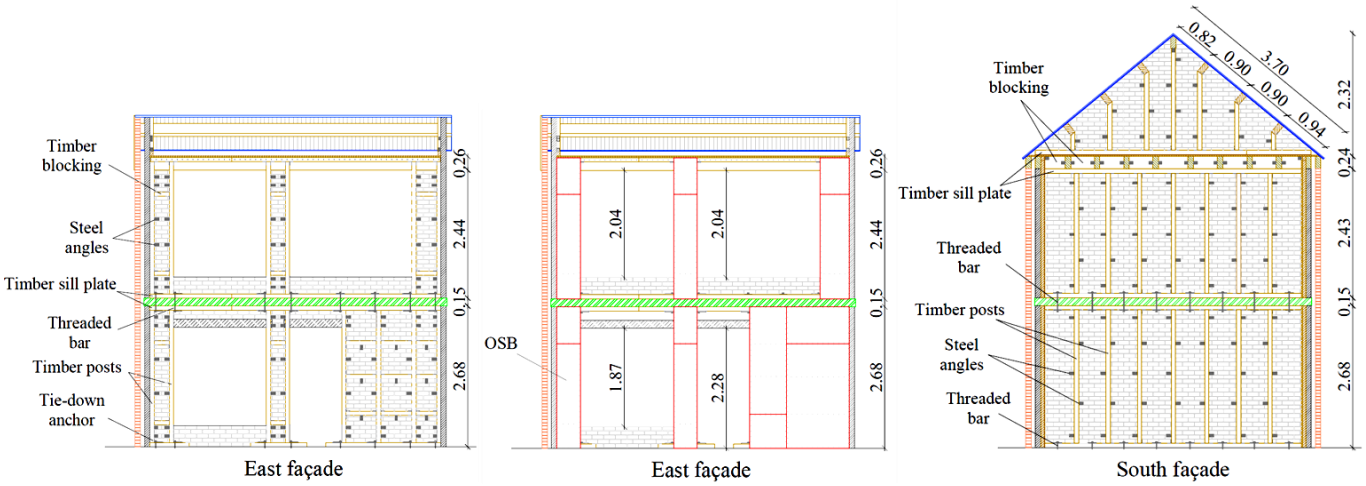

Figure 7. Retrofitted building elevations. Units of m.

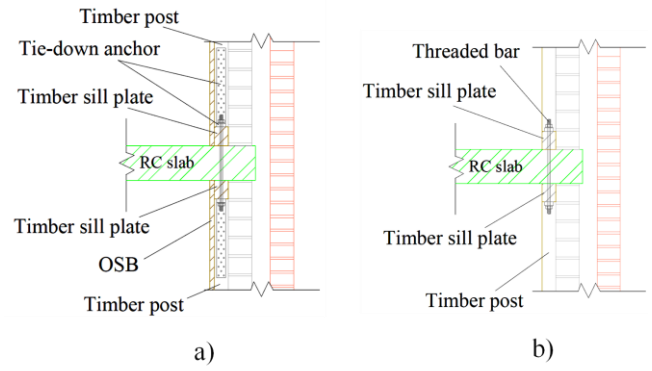

Figure 8. Sill plates-to-RC slab connections details: a) transverse sides (North, South); b) longitudinal sides (East, West).

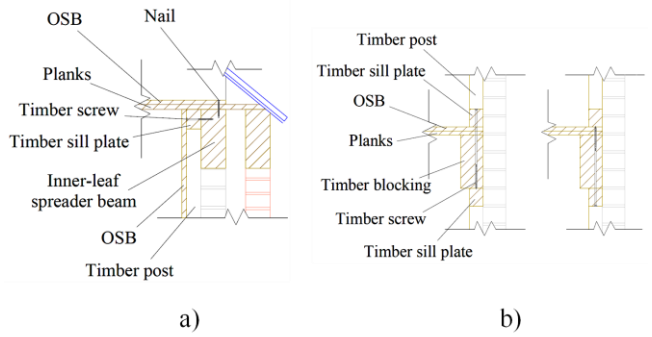

Figure 9. Sill plates-to-timber diaphragm connections details: a) transverse sides (North, South); b) longitudinal sides (East, West).

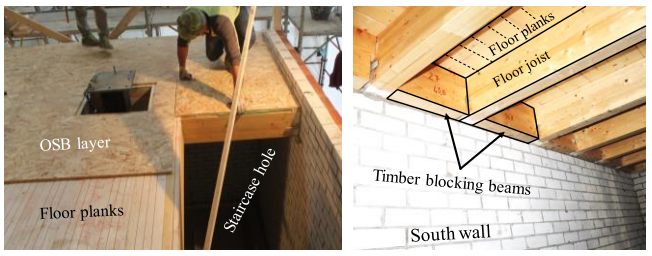

Figure 10. Stiffened timber diaphragm construction details.

3 MECHANICAL PROPERTIES

The experimental campaign included characterization tests performed at the DICAr laboratory of the University of Pavia to determine the mechanical properties of the employed materials, similarly to those performed by Graziotti et al. 2017.

3.1 Masonry

Two characterization test campaigns were performed since the two buildings were built during two different seasons of the year: spring 2018 for the bare building and winter 2018 for the retrofitted one. The calcium silicate and clay masonry compressive strengths (f_m) and secant elastic moduli at 33% of their compressive strength (E_m) were determined according to EN 1052-1 (CEN 1998); the corresponding mortar tensile (f_t) and compressive (f_c) strengths were determined according to EN 1015-11 (CEN 1999). Table 1 shows the obtained results.

The mechanical characterization of wall ties was carried out at Delft University of Technology. The tensile capacity was found to be 4.3 kN, while the pull-out/push-in resistance, when embedded in CS or clay specimens, were 1.25/1.13 kN and 1.94/1.78 kN, respectively (Skroumpelou et al. 2018).

Table 1. Mortar and masonry mechanical properties, bare and retrofitted building.

			Calcium Silicate	C.o.V.	Clay	C.o.V.
Bare	Mortar	f_t [Mpa]	1.74	0.28	0.74	0.5
		f_c [Mpa]	5.06	0.24	2.38	0.47
	Masonry	f_m [Mpa]	10.1	0.06	11.59	0.29
		E_m [Mpa]	6593	0.09	4436	0.44
Retrofitted	Mortar	f_t [Mpa]	1.39	0.38	0.86	0.43
		f_c [Mpa]	3.97	0.41	3.02	0.38
	Masonry	f_m [Mpa]	10.05	0.11	17.62	0.21
		E_m[Mpa]	7319	0.15	5686	0.31

3.2 Retrofit system

The timber employed for vertical posts, horizontal blocking elements and sill plates was solid fir of class S10/C24 according to EN 14081-1 (CEN 2016) with a density of 517 kg/m^3. The specified characteristic compressive strength parallel to fibers was 21 MPa, the characteristic tensile strength parallel to fibers was 14 MPa, and the characteristic Young modulus was 7400 MPa. The selected OSB were classified as OSB/3 according to EN 310 (CEN 1999), with a density of 572 kg/m^3.

Tie-down anchors had a tensile strength of 11.6 kN, while steel angles connecting timber frames to masonry had a shear strength of 3.3 kN (Rothoblaas 2015).

4 INSTRUMENTATION

In order to capture the specimens' experimental behaviour, all tests were monitored by sets of (i) accelerometers, (ii) wire displacement transducers and (iii) linear variable displacement transducers. Moreover, a 3D optical motion acquisition system was employed: passive reflective markers were densely attached to the external surface of the North, South and West clay walls, while high-definition cameras monitored their trajectories.

A highly stiff steel frame was mounted on the shaking table inside both building prototypes providing reference points to measure displacements of the specimens with respect to the shake-table surface, to which the rigid structure was firmly bolted.

Accelerometers were distributed to measure the accelerations: (i) of the shaking-table; (ii) of the walls throughout the buildings' height; (iii) of first floor, second floor, and roof; and (iv) of the internal rigid frame.

Wire potentiometers were used to monitor out-of-plane displacements of the transverse façades with respect to the rigid frame. Linear potentiometers were used to record relative displacements in X, Y and Z directions within the structural system or between structural elements and the shake-table.

5 TESTING PROTOCOLS

The two building prototypes were subjected to a unidirectional seismic excitation of increasing intensity. The incremental dynamic tests were performed by scaling the same single-component input signal aiming at assessing cumulative damage, failure modes and ultimate capacity of the specimens.

A single-component earthquake accelerogram, termed EQ-NPR, with PGA = 0.31g and short significant duration. $D_{s,5\text{-}75}$ = 1.82 s (Figure 11 and Figure 12), was selected upon spectrum-compatibility with the NPR 9998 (NEN 2018) code spectrum, corresponding to an event with return period of 2475 years for the site of Loppersum according to the V4 ground-motion model (Bommer et al. 2017). Table 2 and

Table 3 show the testing protocol applied to the bare and retrofitted buildings, respectively, up to near collapse conditions. The modified Housner intensity (*mHI*, Magenes et al. 2014) and the geometric mean of the pseudo-acceleration spectral ordinates (Bianchini et al. 2009; Kohrangi et al. 2016) were also computed as:

$$mHI = \int_{0.1s}^{0.5s} PSV(T)dT \quad (1)$$

$$PSA_{avg} = \int_{0.3T_1}^{2T_1} \ln PSA\, dT \quad (2)$$

where *PSV* is the pseudo-spectral velocity, *PSA* is the pseudo-spectral acceleration and T_1 is the period of the undamaged specimen.

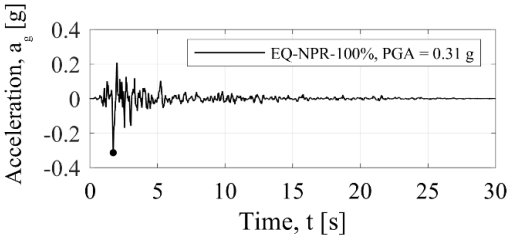

Figure 11. Input signal EQ-NPR at 100% scale factor: acceleration time history.

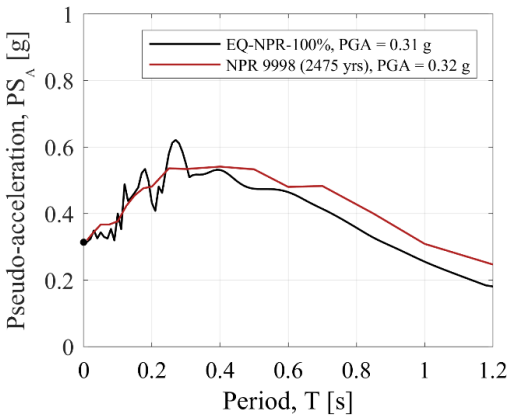

Figure 12. Input signal EQ-NPR at 100% scale factor elastic response spectrum for 5% viscous damping ratio and NPR 9998 elastic spectrum for a return period of 2475 years (Loppersum, Groningen, lat. +53.33, long. +6.75).

Table 2. Bare building: testing protocol and intensity measures.

Input signal	Nominal scale factor	Nom. *PGA* [g]	*PGA* [g]	m*HI* [mm]	PSA_{avg} [g]
EQ-NPR	20%	0.06	0.06	19	0.11
	33%	0.11	0.16	33	0.19
	50%	0.16	0.16	45	0.26
	66%	0.21	0.25	56	0.32
	85%	0.27	0.26	74	0.42
	100%	0.32	0.31	90	0.51
	100%-R†	0.32	0.30	95	0.54
	133%-R †	0.43	0.39	119	0.68

† The input motion was applied with a reversed sign.

Table 3. Retrofitted building: testing protocol and intensity measures.

Input signal	Nominal scale factor	Nom. *PGA* [g]	*PGA* [g]	m*HI* [mm]	PSA_{avg} [g]
EQ-NPR	20%	0.06	0.06	18	0.098
	33%	0.11	0.10	31	0.18
	50%	0.16	0.17	50	0.29
	66%	0.21	0.19	61	0.34
	85%	0.27	0.25	73	0.41
	100%	0.32	0.30	89	0.50
	133%	0.43	0.41	130	0.74
	133%-TR †	0.43	0.43	130	0.73
	166%-TR †	0.53	0.51	150	0.84
	200%-TR †	0.64	0.66	180	1.00
	266%-TR †	0.85	0.78	220	1.30

† The roof structure was restrained with steel rods against longitudinal displacements.

6 TEST RESULTS

Two different types of response to earthquake excitation were observed on the two specimens. The bare building was characterized by a local response of the second-floor timber diaphragm, which slid on top of the masonry walls preventing attainment of the full in-plane resistance of the piers. Instead, the retrofitted building exhibited a global "box-type" behavior with increased in-plane and out-of-plane capacities of the masonry piers thanks to the enhancement of connections between walls and floor diaphragms.

The following paragraphs compare the damage to the building specimens after testing under EQ-NPR-100% and at ultimate conditions. In Figure 13 through Figure 18, Figure 21, and Figure 22, red lines refer to the cracks developed during the considered run, black lines refer to the cracks accumulated during previous runs.

6.1 Damage comparison after EQ-NPR-100% (PGA = 0.3g)

The damage cumulated by the two prototypes after testing at EQ-NPR-100% was significantly different.

In the bare building, damage was mainly concentrated at the second storey. The lack of connections between masonry and second-floor timber diaphragm allowed sliding to occur, increasing the displacement demand at that storey. Looking at the damage pattern of the East wall presented in Figure 13, it can be seen that the sliding crack between the inner-leaf spreader beam and the masonry was fully developed, denoting a complete loss of the cohesion contribution to the connection capacity. Consequently, the second-storey piers resistance could not be engaged. The transverse walls tended to displace out of plane, following the second-floor diaphragm, and involved the slender return walls of the longitudinal facades. The North transverse wall tended to detach from the second storey squat pier with a vertical crack forming along the North-West corner. The significant difference in displacement demand that occurred between first and second storey can be clearly seen on the North-side inner leaf (Figure 13): widespread damage accumulated at the second storey while the first one was almost intact. The same conclusion can be made by looking the crack pattern evidenced on the North clay façade (Figure 14).

Focusing on the retrofitted building (Figure 15 and Figure 16), the accumulated damage was significantly lower. Only hairline cracks were detected on the inner leaves (Figure 15): at the roof-gable system, which was demonstrated to be

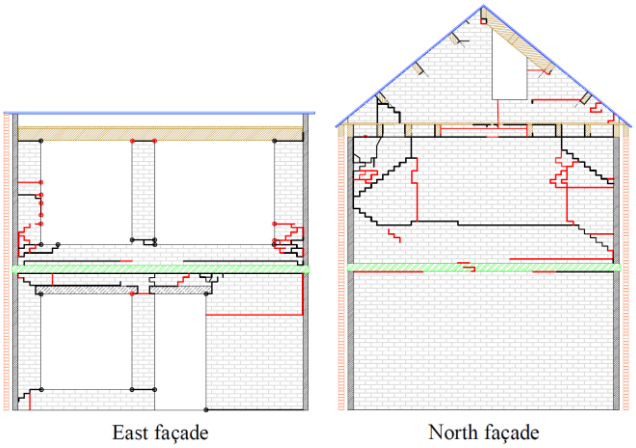

Figure 13. Bare building crack pattern after EQ-NPR-100%: CS inner leaves.

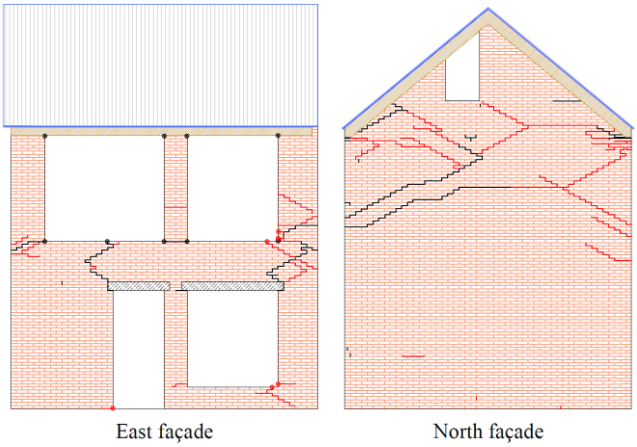

Figure 14. Bare building crack pattern after EQ-NPR-100%: clay external veneers.

particularly flexible in this typology of buildings (Graziotti et al 2017); and on the South side, due to the interaction between second-floor timber beams and the supporting CS wall. Also the clay outer leaves presented minor damage (Figure 16), hairline cracks were detected at the interfaces between spreader beams and masonry, between lintels and masonry, and between roof purlins and masonry.

6.2 Damage comparison at ultimate conditions

The last test run for the bare building was performed under EQ-NPR-133%-R (PGA = 0.4g). The specimen showed heavy damage at the second storey, while limited damage developed at the first one on both inner and outer leaves (Figure 17 and Figure 18). No new mechanisms were activated and the distribution of cracks was very similar to the one observed after EQ-NPR-100%. However, residual crack widths increased significantly (up to 50 mm) and the structure at the end of the test was very close to loose static stability. Figure 19 shows the accumulated crack width between the second storey squat-pier (West side) and the transverse wall (North side). Figure 20 depicts the developed

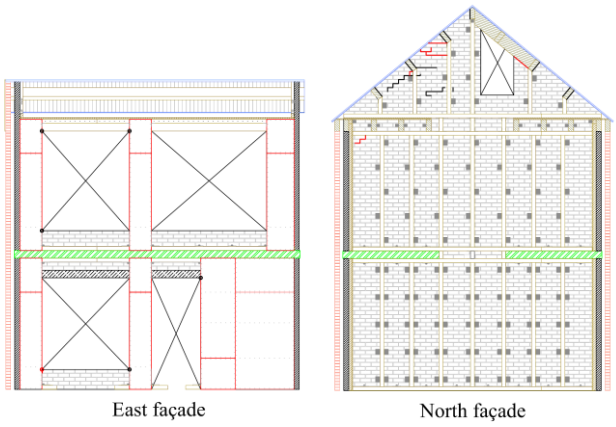

Figure 15. Retrofitted building crack pattern after EQ-NPR-100%: CS inner leaves transverse walls.

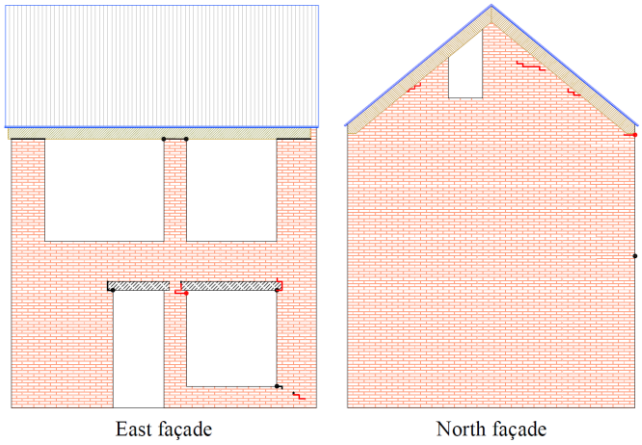

Figure 16. Retrofitted building crack pattern after EQ-NPR-100%: clay external veneers.

damage of the first storey squat wall of the East façade at the corner with the South transverse wall.

A completely different ultimate state was reached by the retrofitted building (Figure 21 through Figure 23), which was able to sustain the applied ground motion up to EQ-NPR-266% (PGA = 0.8g). The timber retrofit system allowed a full exploitation of the masonry capacity due to the enhancement of connections and of the in-plane and out-of-plane resistances of the walls. Remarkably, the adopted strengthening measures led the building to develop a torsional response that allowed to take advantage of the in-plane resistance of the first-storey transverse walls.

As opposed to the bare building, the CS inner leaves were heavily damaged at the first storey, with significant residual crack widths (up to 35 mm), while the second storey showed diffuse damage yet with only hairline cracks (Figure 21 and Figure 23). Looking at the clay veneer of the North façade, widespread damage could be observed throughout the whole height (Figure 22) rather than concentrated at the second storey.

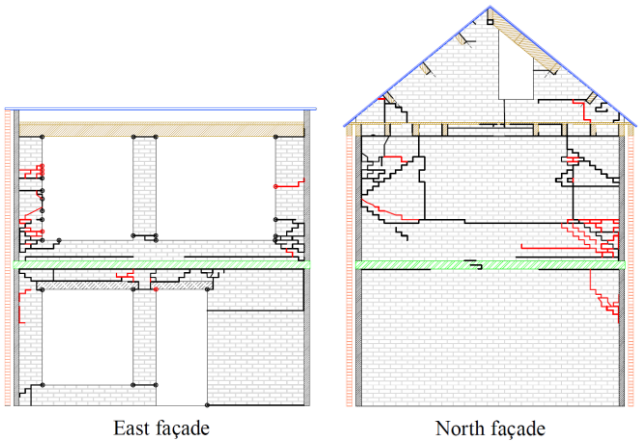

Figure 17. Bare building crack pattern at ultimate conditions: CS inner leaves.

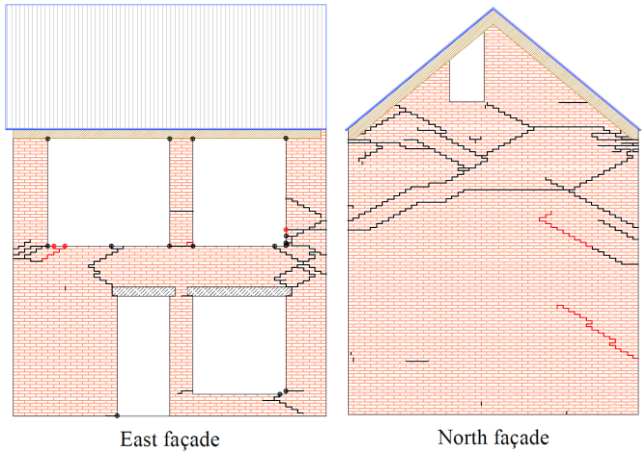

Figure 18. Bare building at ultimate conditions: longitudinal clay outer leaves.

Figure 19. Bare building at ultimate conditions: second storey North-West corner.

Figure 20. Bare building at ultimate conditions: first storey South-East corner.

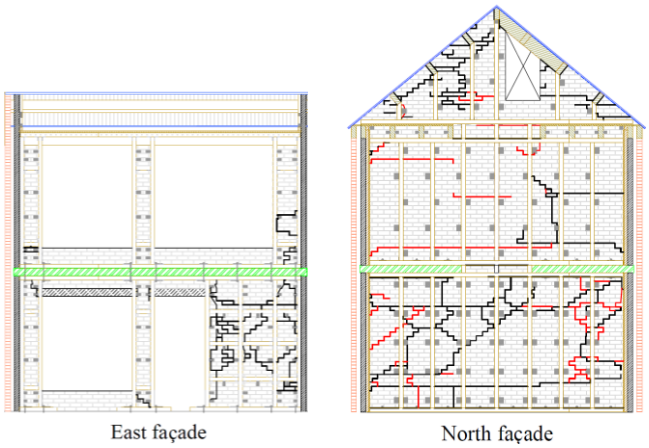

Figure 21. Retrofitted building crack pattern at ultimate conditions: CS inner leaves.

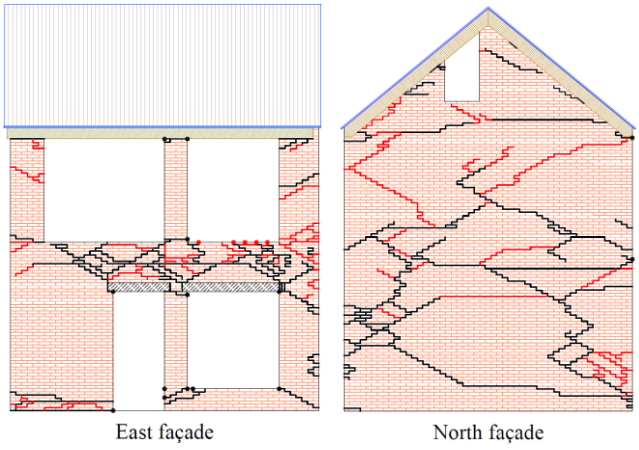

Figure 22. Retrofitted building crack pattern at ultimate conditions: clay outer leaves.

Figure 23. Retrofitted building at ultimate conditions: transverse walls.

7 CONCLUSIONS

This paper discussed two incremental dynamic tests performed on two full-scale unreinforced masonry (URM) cavity-wall buildings with the same geometrical features, one in bare conditions and one in retrofitted configuration. A light timber strengthening system consisting of timber frames

with nailed oriented-strands boards was installed on the internal surface of the inner loadbearing masonry leaf.

The specimens were pushed to their near collapse limit state by scaling the same ground motion, representative of the induced seismicity of the Groningen region of The Netherlands.

Applying the input signal corresponding to an event with return period of 2475 years for the area (PGA = 0.3g), the bare building developed a local mechanism. This was characterized by sliding of the second-floor timber diaphragm on top of the second-storey masonry piers, causing concentration of damage at the second storey while the first one was almost intact. Instead, the same run caused only minor cracks to the retrofitted building, which responded globally to the seismic excitation.

The bare and retrofitted buildings sustained a maximum PGA of 0.4g and 0.8g, respectively, reaching near-collapse damage conditions. The bare specimen exhibited a similar behaviour as observed during the run with PGA = 0.3g, but with significant increments of crack widths. The strengthened building, instead, showed a global response up to the end of the test.

The combined improvements of connections and piers capacity allowed the retrofitted building to develop a torsional response that fully exploited the strength of all structural elements, including the in-plane resistance of the transverse squat walls. Damage was fairly distributed throughout the building.

Numerical simulations for vulnerability models of original and retrofitted houses, cost/benefit analyses of this solution, and extension of this retrofit to other URM building typologies, will be considered in next future based on these results.

8 ACKNOWLEDGEMENTS

This work is part of the EUCENTRE project "Study of the vulnerability of masonry buildings in Groningen", within the research programme framework on hazard and risk of induced seismicity in the Groningen province, sponsored by the Nederlandse Aardolie Maatschappij BV (NAM). The data post-processing was also partially funded by the DPC-ReLUIS within the framework of the Work-Package-5 2019-2021: "interventi di rapida esecuzione a basso impatto ed integrati". The authors would like to thank all parties involved in this project: the DICAr Laboratory of the University of Pavia and the EUCENTRE Laboratory, which performed the tests, the DPC-ReLUIS and the partner NAM. The valuable advice of R. Pinho, G. Magenes and A. Penna was essential to the project and is gratefully acknowledged.

REFERENCES

American Wood Council (AWC), 2008. ANSI/AF&PA SDPWS-2008: Special design provisions for wind and seismic. Washington, D.C.

Bianchini, M., Diotallevi, P., Baker, J.W., 2009. Prediction of inelastic structural response using an average of spectral accelerations. *In Proceedings of the 10th International Conference on Structural Safety and Reliability* (ICOSSAR09), Osaka, Japan.

Bommer, J. J., Dost, B., Edwards, B., Stafford, P. J., van Elk, J., Doornhof, D., Ntinalexis, M., 2015. Developing an application-specific ground-motion model for induced seismicity. *Bulletin of the Seismological Society of America*, **106**(1), 158-173.

Bommer, J.J., Dost, B., Edwards, B., Kruiver, P.P., Meijers, P., Ntinalexis, M., Rodriguez-Marek, A., Ruigrok, E., Spetzler, J., Stafford, P.J., 2017. V4 ground-motion model (GMM) for response spectral accelerations, peak ground velocity, and significant durations in the Groningen field. *Research Report submitted to NAM*.

Bourne, S. J., Oates, S. J., Bommer, J. J., Dost, B., Van Elk, J., & Doornhof, D., 2015. A Monte Carlo Method for Probabilistic Hazard Assessment of Induced Seismicity due to Conventional Natural Gas Production. *Bulletin of the Seismological Society of America*, **105**(3), 1721-1738.

Crowley, H., Pinho, R., van Elk, J., & Uilenreef, J., 2018. Probabilistic damage assessment of buildings due to induced seismicity. *Bulletin of Earthquake Engineering*, 1-22.

Damiani, N., Miglietta, M., Mazzella, L., Grottoli, L., Guerrini, G., Graziotti, F., 2019. Full-scale shaking table test on a Dutch URM cavity-wall terraced-house end unit – A retrofit solution with strong-backs and OSB boards – EUC-BUILD-7. EUCENTRE foundation, Pavia, ITA, Research report EUC052/2019U.

European Committee for Standardization (CEN), 1998. EN 1052-1: Methods of test for masonry - Part 1: Determination of compressive strength. European Committee for Standardization, Brussels, Belgium

European Committee for Standardization (CEN), 1999. EN 1015-11: Methods of test for mortar for masonry - Part 11: Determination of flexural and compressive strength of hardened mortar. European Committee for Standardization, Brussels, Belgium.

European Committee for Standardization (CEN), 1999. EN 310: Wood based panels. Determination of modulus of elasticity in bending and of bending strength. European Committee for Standardization, Brussels, Belgium.

European Committee for Standardization (CEN), 2016. EN 14081-1: Timber Structures. Strength graded structural timber with rectangular cross section. Part I: General requirements.. European Committee for Standardization, Brussels, Belgium.

Graziotti, F., Rossi, A., Mandirola, M., Penna, A., & Magenes, G., 2016a. Experimental characterization of calcium-silicate brick masonry for seismic assessment. *In Brick and block masonry: trends, innovations and challenges—proceedings of the 16th international brick and block masonry conference, IBMAC* (pp. 1619-1628).

Graziotti, F., Tomassetti, U., Penna, A., & Magenes, G., 2016b. Out-of-plane shaking table tests on URM single leaf and cavity walls. *Engineering Structures*, **125**, 455-470.

Graziotti, F., Tomassetti, U., Kallioras, S., Penna, A., & Magenes, G., 2017. Shaking table test on a full scale URM cavity wall building. *Bulletin of earthquake engineering*, **15**(12), 5329-5364.

Graziotti, F., Penna, A., & Magenes, G., 2018. A comprehensive in situ and laboratory testing programme supporting seismic risk analysis of URM buildings subjected to induced earthquakes. *Bulletin of Earthquake Engineering*, 1-25.

Graziotti, F., Tomassetti, U., Sharma, S., Grottoli, L., & Magenes, G., 2019. Experimental response of URM single leaf and cavity walls in out-of-plane two-way bending generated by seismic excitation. *Construction and Building Materials*, **195**, 650-670.

Jafari, S., Rots, J. G., Esposito, R., & Messali, F., 2017. Characterizing the material properties of Dutch unreinforced masonry. *Procedia engineering*, **193**, 250-257.

Kallioras, S., Guerrini, G., Tomassetti, U., Marchesi, B., Penna, A., Graziotti, F., & Magenes, G., 2018. Experimental seismic performance of a full-scale unreinforced clay-masonry building with flexible timber diaphragms. *Engineering Structures*, **161**, 231-249.

Kallioras, S., Graziotti, F., & Penna, A., 2019. Numerical assessment of the dynamic response of a URM terraced house exposed to induced seismicity. *Bulletin of Earthquake Engineering*, **17**(3), 1521-1552.

Kohrangi, M., Bazzurro, P., Vamvatsikos, D., 2016. Vector and scalar IMs in structural response estimation, Part I: Hazard analysis. *Earthquake Spectra*, **32**(3):1507-1524. DOI: 10.1193/053115EQS080M.

Magenes, G., Penna, A., Senaldi, I. E., Rota, M., & Galasco, A., 2014. Shaking table test of a strengthened full-scale stone masonry building with flexible diaphragms. *International Journal of Architectural Heritage*, **8**(3), 349-375.

Malomo, D., Pinho, R., Penna, A., 2018. Using the applied element method for modelling calcium silicate brick masonry subjected to in-plane cyclic loading. *Earthquake Engineering & Structural Dynamics*, **47**(7), 1610-1630.

Messali, F., Ravenshorst, G., Esposito, R., & Rots, J., 2017. Large-scale testing program for the seismic characterization of Dutch masonry walls. In *Proceedings of the 16th World Conference on Earthquake Engineering*, 16WCEE, Santiago, CL.

Miglietta, M., Mazzella, L., Grottoli, L. Guerrini, G., Graziotti, F., 2018. Full-scale shaking table test on a Dutch URM cavity-wall terraced-house end unit – EUC-BUILD-6. EUCENTRE foundation, Pavia, ITA, Research report EUC160/2018U.

Netherlands Standardization Institute (NEN), 2018. Assessment of structural safety of buildings in case of erection, reconstruction, and disapproval - Basic rules for seismic actions: induced earthquakes (NPR 9998). Netherlands Standardization Institute, Delft, The Netherlands (in Dutch).

Rothoblaas catalogue, 2015: Wood connectors and timber plates, Screws for wood. https://www.rothoblaas.com/catalogue-rothoblaas

Rots, J. G., Messali, F., Esposito, R., Mariani, V., & Jafari, S., 2017. Multi-scale approach towards Groningen masonry and induced seismicity. Key Engineering Materials, 747, 653-661.

Skroumpelou, G., Messali, F., Esposito, R., & Rots, J. G., 2018. Mechanical characterization of wall tie connection in cavity walls. In 10th Australian masonry conference, Sydney, Australia.

Tomassetti, U., Graziotti, F., Penna, A., & Magenes, G., 2018. Modelling one-way out-of-plane response of single-leaf and cavity walls. *Engineering Structures*, **167**, 241-255.

van Elk, J., Bourne, S. J., Oates, S. J., Bommer, J. J., Pinho, R., Crowley, H., 2019. A probabilistic model to evaluate options for mitigating induced seismic risk. *Earthquake Spectra*, **35**(2), 537-564.